Proceedings of the 10th Brazilian Congress of Thermal Sciences and Engineering -- ENCIT 2004
Braz. Soc. of Mechanical Sciences and Engineering -- ABCM, Rio de Janeiro, Brazil, Nov. 29 -- Dec. 03, 2004

Paper CIT04-0485

CFD EVALUATION OF THE DISCHARGE COEFFICIENT OF AIR OUTLETS IN THE PRESENCE OF AN EXTERNAL FLOW

Antonio Batista de Jesus
Embraer – Empresa Brasileira de Aeronáutica S/A
antonio.jesus@embraer.com.br

Viviam Lawrence Takase
Embraer – Empresa Brasileira de Aeronáutica S/A
Viviam.lawrence@embraer.com.br

Harry T. Maia Vinagre
Embraer – Empresa Brasileira de Aeronáutica S/A
harry.vinagre@embraer.com.br

Abstract. *In this work, CFD analysis is used to evaluate the discharge coefficients of air outlets in the presence of an external flow with or without grills in the outlet region. In a first step, a CFD model was built in a configuration similar to one for which there are experimental data available in the open literature. The discharge coefficients curve of an outlet without grills in the presence of an external flow was obtained numerically and the results were found to be in good agreement with experimental data.In a second step, it was evaluated the effect of the external flow Mach number and the presence of vanes in the outlet region in the discharge coefficient. Two cases were considered: one with internal vanes and another with external vanes. It was concluded that, comparing to the case analyzed in step one, the external Mach number has little influence in the discharge coefficient values, the internal vanes were verified not to alter the discharge coefficient values in the regions of lower mass flow rates, but to reduce the discharge coefficient for the higher massflow rates conditions, while the external vanes were verified to substantially increase the discharge coefficients in the lower mass flow rates conditions, but also to reduce the discharge coefficients in high mass flow rate cases.*

Keywords*. Air outlets, discharge coefficients, jets, crossflow, CFD.*

1. Introduction

The design of aircraft air-conditioning and ventilation systems starts with the definition of an airflow rate requirement which is followed by three important tasks: the definition of the air source, the calculation of the pressures losses involved and the determination of the outlet regions, where the airflow is discharged in the freestream. Generally, the air source consists of air inlets, which are designed for recovering an amount of the external flow dynamic pressure. The pressure recovery of the air inlets should be enough for overcoming the pressure losses, such that the resulting airflow rate is adequate.

In this scenario, the definition of the air outlets type and positioning may be regarded as a secondary task in the design process. However, this statement is easily proved to be wrong when it is considered that in aircraft ventilation and air-conditioning systems, the outlet pressure losses, which are expressed as a discharge coefficient, may be orders of magnitude higher than internal losses. In addition, as the air outlets are located on the aircraft surface, the design should consider the drag produced by the outlets, along with installation aspects as protection against foreign-object damage (FOD) caused, for example, by debris or water.

The drag and installation aspects mentioned above lead to a general characteristic of aircraft air outlets, which is the presence of grills. Grills that are installed in an air outlet in an aircraft may be flush or with vanes, which can also be internal or external. Due to the many possible geometric configurations, CFD is a valuable tool in the analysis of the airflow discharging into a freestream through outlets with grills.

This work deals with the use of CFD analysis in the determination of the discharge coefficients of air outlets with or without grills, which may be in configurations with internal or external vanes. At first, it was performed a comparison between CFD calculated and experimental results (wind-tunnel) for the discharge coefficients in a configuration of an outlet without grills discharging in a freestream. It was also evaluated the effect of varying the freestream Mach number in the discharge coefficients values. In a second step, it was calculated the discharge coefficient for the same outlet of the first analysis, but including internal and external vanes. At last, it was checked the accuracy of the CFD analysis in capturing local phenomena by means of comparing experimental values of the pressure coefficient in the regions before and after the air outlet with numerical results.

The phenomena of jets discharging in crossflows has been subject of extensive research by either numerical or experimental methods, due to many applications as turbine blade cooling, enhancement of mixing in combustors and vertical take-off and landing (VTOL) aircraft. A great emphasis has been placed in understanding the local phenomena

that occur in the mixing process of the two flows, particularly in the identification of the vortex pairs that are formed (Fric and Roshko, 1994; Kelso et al., 1996).

However, it is not commonly found in the open literature, studies concerning the design of auxiliary air outlets for aircraft ventilation/air-conditioning systems, and most type of those are experimental papers, which describe wind-tunnel tests results obtained in the 50's. Particularly, it has been of great use the works of Dewey (1955) and Dewey and Vick (1955), who evaluated the discharge coefficients of many configurations of auxiliary outlets, discharging in a freestream of speeds commonly found in commercial and military aircraft. Those data have been largely used and became part of important handbooks as the SAE Handbook of Aerospace Sciences (1990).

In the works of Dewey (1955) and Dewey and Vick (1955), many types of outlets were installed on a flat plate, instrumented and tested while discharging in the wind-tunnel flow in several configurations. It was measured the discharge coefficient of the outlets, along with the pressure coefficient at the flat plate region just before and after the outlet and also a thrust coefficient for evaluation of the drag produced. Those works, however, dealt with flush or recessed outlets, but not including the effects of grills, which are commonly installed in an aircraft.

The present work is aimed at studying the effects of grills in the discharge coefficients of auxiliary air outlets. CFD is used as a tool for such evaluation. At first, it is used a CFD model to reproduce the results of Dewey's works dealing with fliush outlets. In a second phase, it was evaluated the discharge coefficients curve of configurations similar to what was studied in the first step, but with grills installed on them.

Results are presented in terms of discharge coefficients curves for the configurations with and without grills, the latter are compared to experimental data of Dewey and Vick (1955). The pressure coefficient values at the flat plate region before and after the outlet are also compared to experimental values of the same reference, in the outlet without any grill configuration.

3. Development

The basic configuration chosen for the present analysis is a rectangular (square) duct, which discharges air normally to a flat plate, on which there is another air crossflow. The square duct of cross-sectional area 0.7056 m^2 and length 5.08 m is positioned at the center of a 43.18 m x 15.875 m flat plate. Those dimensions are proportional to a similar configuration tested in wind-tunnel by Dewey and Vick (1955).

The computational domain defined for the present analysis consists of a rectangular box, which in the longer bottom side has a square normal duct. A 43.18 m x 15.875 m x 11.43 m box represents the domain in which the freestream flows, as it is illustrated in Fig. 01. The freestream flow enters through one side of the box, crosses the outlet and leaves at the other side. Simultaneously, air comes into through the bottom part of the duct and is discharged in the freestream, leaving through the same face.

Three types of geometric models were evaluated: the first one with a simple duct outlet, without any grills, similar to what was in Dewey and Vick (1955), the second one with the same geometry but a set of internal vanes. The vanes represent a grill and are oriented 60^o in the freestream flow direction. The third model also has 60^o oriented vanes, but in this case the vanes are not flush to the flat plate, which is aimed to generate suction effects that could improve the outlet performance, with the penalty of drag increment. Figure 02 shows a zoom view at the duct outlet of the three configurations being analyzed, without any grill, a grill with internal vanes and a grill with external vanes. The thickness of each vane is 0.1 m for the internal vane and 0.2 m for the external vane (the flat plate divides the external vanes in the middle).

The CFD++ v.3.5.1 commercial CFD tool from Metacomp Technologies was used for solving all cases. It is a finite volume solver, which uses a coupled method of solution of the continuity, momentum and energy equations, with the option of pre-conditioning in low speed conditions. In the present analysis, it was used RANS calculations, with a realizable k-epsilon turbulence model.

Second-order spatial discretizations were used in all cases. More details about the CFD++ code structure may be found in the works of Chakravarthy et al. (2000) and Jesus et al. (2002). Convergence was monitored by the normalized residuals of the continuity, momentum, energy and turbulence quantities equations. The residuals dropped at least 4 orders of magnitudes in all cases. It was also certified that the mass flow rate through the air outlet had reached a converged value in all calculations.

The governing equations of this problem are the Reynolds-Averaged equations of continuity (Eq. 1), momentum (Eq. 2) and energy (Eq. 3) with the assumption of ideal gas:

$$\frac{\partial \overline{\rho}}{\partial t} + \frac{\partial \left(\overline{\rho} U_k \right)}{\partial x_k} = 0 \tag{1}$$

$$\frac{\partial \left(\overline{\rho} U_i \right)}{\partial t} + \frac{\partial \left(\overline{\rho} U_i U_k \right)}{\partial x_k} = -\frac{\partial \overline{p}}{\partial x_i} + \frac{\partial}{\partial x_k} \left[\overline{\tau}_{ik} - \overline{\rho u_i u_k} \right] \tag{2}$$

$$\frac{\partial\left(\bar{\rho}E\right)}{\partial t}+\frac{\partial\left(\bar{\rho}E+\bar{p}\right)U_k}{\partial x_k}=-\frac{\partial}{\partial x_k}\left(c_p\overline{\rho T'' u_k}+\bar{q}_k\right)+\frac{\partial}{\partial x_k}\left(-\bar{\rho}_i U_i\overline{u_i u_k}+U_i\bar{\tau}_{ik}\right)+\frac{\partial}{\partial x_k}\left(-\frac{1}{2}\overline{\rho u_j u_j u_k}+\overline{u_i\tau_{ik}}\right) \quad (3)$$

where: c_p – specific heat of air, J/(kg.K)
E – mean total energy per unit mass (Favre average), J/kg
p – pressure, Pa
q – heat-flux vector, W/m^2
T'' – temperature fluctuation (related to Favre average), K
t – time, s
U – mean velocity (Favre average), m/s
u – velocity fluctuation (related to Favre average), m/s
x – spatial coordinate, m
ρ - density, kg/m^3
τ - shear stress, N/m^2
$\bar{(\,)}$ - time-averaged quantities

Turbulence modeling was provided by CFD++'s two equation realizable k-ε model, that solves transport equations for the turbulence kinetic energy k and its dissipation rate ε. The realizable k-ε model is a variant of the standard k-ε model which introduces modifications to overcome some weaknesses of the standard model. The realizable model accounts for certain known physical properties of the stress tensor by introducing a bound on the magnitude of the predicted tensor components, which improves predictive accuracy and has a beneficial effect on stability.

The turbulent transport equations are as follows:

$$\frac{\partial\left(\bar{\rho}k\right)}{\partial t}+\frac{\partial\left(\bar{\rho}U_k k\right)}{\partial x_k}=\frac{\partial}{\partial x_k}\left[\left(\mu+\frac{\mu_t}{\sigma_k}\right)\frac{\partial k}{\partial x_k}\right]+P_k-\bar{\rho}\varepsilon \quad (4)$$

$$\frac{\partial\left(\bar{\rho}\varepsilon\right)}{\partial t}+\frac{\partial\left(\bar{\rho}U_k \varepsilon\right)}{\partial x_k}=\frac{\partial}{\partial x_k}\left[\left(\mu+\frac{\mu_t}{\sigma_\varepsilon}\right)\frac{\partial \varepsilon}{\partial x_k}\right]+\left(c_{\varepsilon 1}P_k-c_{\varepsilon 2}\bar{\rho}\varepsilon+E\right)T_t^{-1} \quad (5)$$

where,

$$T_t=\frac{k}{\varepsilon}\max\left\{1,\xi^{-1}\right\} \quad (6)$$

where $\xi=\sqrt{R_t/2}$ with $R_t=\rho k^2/(\mu\varepsilon)$.

The Boussinesq relation is used to obtain the Reynolds-stresses from the modeled eddy viscosity μ_t and the available mean-strain tensor:

$$\overline{\rho u_i u_j}=\frac{2}{3}\delta_{ij}\rho k-\mu_t S_{ij} \quad (7)$$

where,

$$S_{ij}=\frac{1}{2}\left(\frac{\partial U_i}{\partial x_j}+\frac{\partial U_j}{\partial x_i}-\frac{2}{3}\frac{\partial U_k}{\partial x_k}\frac{\partial U_k}{\partial x_k}\delta_{ij}\right) \quad (8)$$

Full details of this model, including all model terms and constants can be found in Chakravarthy et al. (2000).

For all those three geometric models mentioned above, a 3D computational mesh was generated using ICEM CFD hexahedral mesh generator. The same mesh was used in all calculations with the vanes treated as walls or interior (flow-through) surfaces, depending on the desired configuration. The mesh had about 800,000 elements mostly concentrated in the region around the air outlet, particularly in the wake. It was also put a great emphasis in solving the wall effects in turbulence quantities by means of a very refined mesh in the region close to the flat plate. Figure 03 brings a view of the computational mesh used, including the location where boundary conditions were imposed.

The mesh takes advantage of the symmetry of the problem, with the definition of a symmetry plane. This boundary condition imposes a symmetry condition on the flow, in which all scalar and vector quantities are considered to be

mirror-imaged in the planes defined by the surface-boundary faces. The flow velocity experiences a free slip at the boundary, becoming tangential to the surface on the boundary itself.

The box faces painted in pink were set for a characteristics-based boundary condition, where it was imposed values for the freestream static pressure, static temperature, Mach number and flow direction. This boundary condition takes a specified set of free-stream data, but rather than using this data directly, a Riemann problem is solved at the boundary, using the supplied data as a virtual state outside the domain. The resulting interface values from the Riemann solution are then used to compute the interface flux.

The flat plate and the vanes (in the cases with a grill) were modeled as viscous walls, using wall functions. This boundary condition models a solid wall surface, but uses an assumed log-law to impose the wall shear-stress and determine the turbulence production in the near-wall cell.

The duct was modeled as an inviscid wall in order to guarantee that the discharge coefficient evaluated is only related to the outlet losses. This boundary condition is exactly equivalent to that of the symmetry condition.

The duct inlet surface was modeled as a subsonic reservoir boundary, where it was imposed a total pressure and total temperature. The flow direction was defined as normal to the duct inlet. The inflow velocity is directly extrapolated from the interior, whilst the inflow pressure and temperature are determined by assuming isentropic relations hold across the inlet.

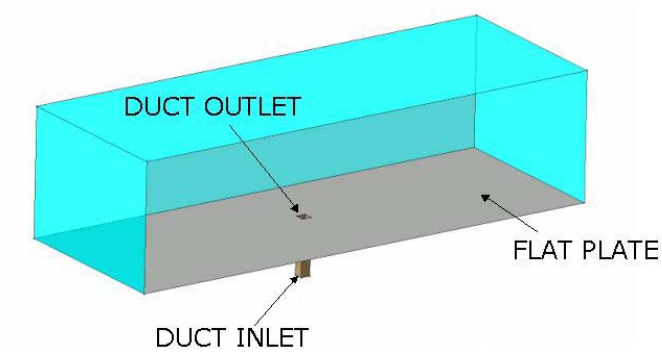

Figure 01. CFD model geometry.

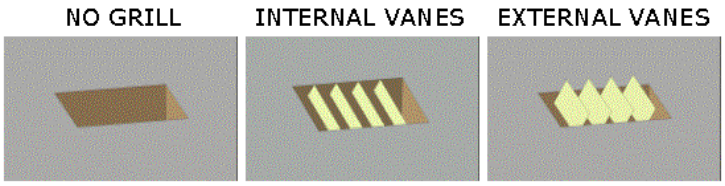

Figure 02. Outlet Geometries.

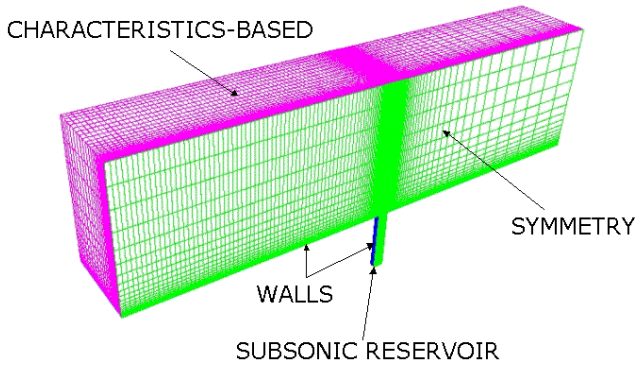

Figure 03. CFD mesh and boundary conditions location.

For the case without grill experimental results are available from Dewey and Vick (1955). A total of 10 simulations were run considering this geometry for different external flow regimes and for different conditions at the duct inlet.

Table 01 lists the boundary conditions used in the case of an outlet without a grill. It was considered high-speed and low-speed values of the external flow. The total pressure values at the duct outlet were chosen to cover a wide range of points in the discharge coefficient curve.

Table 01 – List of Simulated Cases for the Outlet without Grill.

	Duct Inlet		External Flow		
	Total Pressure (Pa)	Total Temperature (K)	Static Pressure (Pa)	Static Temperature (K)	Mach Number (-)
Case1	104000	288	101325	288	0.7
Case2	108000	288	101325	288	0.7
Case3	114153	288	101325	288	0.7
Case4	115131	288	101325	288	0.7
Case5	120000	288	101325	288	0.7
Case6	125000	288	101325	288	0.7
Case7	130000	288	101325	288	0.7
Case8	102000	288	101325	288	0.3
Case9	104000	288	101325	288	0.3
Case10	106000	288	101325	288	0.3

The experimental results of Dewey an Vick (1955) are presented in terms of a discharge coefficient curve as a function of the so-called mass flow ratio, which consists in the ration between the mass flow rate flowing trough the duct outlet (which is a result of the calculation) and the mass flow rate that would result through a flow at the same freestream condition (in terms of density and velocity) in the outlet duct. The mass-flow ratio is defined by the following expression:

$$MFR = \frac{\dot{m}_{actual}}{\rho_\infty V_\infty A_{outlet}} \tag{9}$$

The duct mass flow rate is a result of the simulation and is used to determine the discharge coefficient, calculated by:

$$C_D = \frac{\dot{m}_{actual}}{\dot{m}_{ideal}} \tag{10}$$

where, for each case the ideal outlet flow is calculated by the well-known of isentropic mass flow rate as a function of total temperature, total pressure and Mach number:

$$\frac{\dot{m}_{ideal}}{A_{outlet}} = \sqrt{\frac{\gamma}{R}} \cdot \frac{P_T^{inlet}}{\sqrt{T_T^{inlet}}} \cdot \frac{M}{\left(1 + \frac{\gamma - 1}{2} M^2\right)^{\frac{\gamma+1}{2(\gamma-1)}}} \tag{11}$$

and, the ideal Mach number is evaluated from the total pressure at the duct inlet and the freestream static pressure:

$$M = \sqrt{\frac{\left(\frac{P_T^{inlet}}{P^{outlet}}\right)^{\frac{\gamma-1}{\gamma}} - 1}{\frac{\gamma-1}{2}}} \tag{12}$$

After running the cases without grills, it was considered the cases with internal and external vanes. The same computational mesh and numerical parameters were adopted for all cases. The main difference from the case without grills was that the vanes surfaces, which were interior surfaces, were turned into walls. Cases 1, 4, 6 and 7, from Tab. 01, were run for both the internal and external vanes conditions. The discharge coefficient values, as a function of the mass flow ratio were obtained for both configurations and compared to the case without grills. Next section brings the results obtained.

3. Results and Discussion

Table 02 lists the results obtained for the simulations without grill in terms of mass flow rate through the air outlet, the mass flow ratio and the discharge coefficient obtained. Cases 1 to 7 refer to a Mach 0.7 external flow, while cases 8,9 and 10 the freestream is at Mach 0.3.

Table 02– Summary of Results for Configuration without any Grill.

	Actual Discharge Flow (kg/s)	Mass Flow Ratio (-)	Discharge Coefficient (-)
Case1	7.77	0.038	0.136
Case2	20.64	0.100	0.229
Case3	50.20	0.244	0.403
Case4	53.56	0.260	0.415
Case5	100.48	0.488	0.670
Case6	141.72	0.688	0.841
Case7	170.24	0.827	0.919
Case8	5.37	0.061	0.187
Case9	31.44	0.356	0.551
Case10	68.94	0.781	0.914

The work of Dewey and Vick (1955) brings experimental results for the Mach 0.7 flow and Fig. 04 shows a comparison between present numerical and their experimental values. Although, Dewey and Vick (1955) work plots a curve, actual experimental points were those shown in Fig. 04. It can be observed a better agreement between numerical and experimental values for the lower and higher mass flow ratios conditions. In the mid-values, it is noticed an approximately 10% deviation between CFD and wind tunnel values. It can also be observed that the discharge coefficient increases with mass flow ratio, approaching a free jet condition.

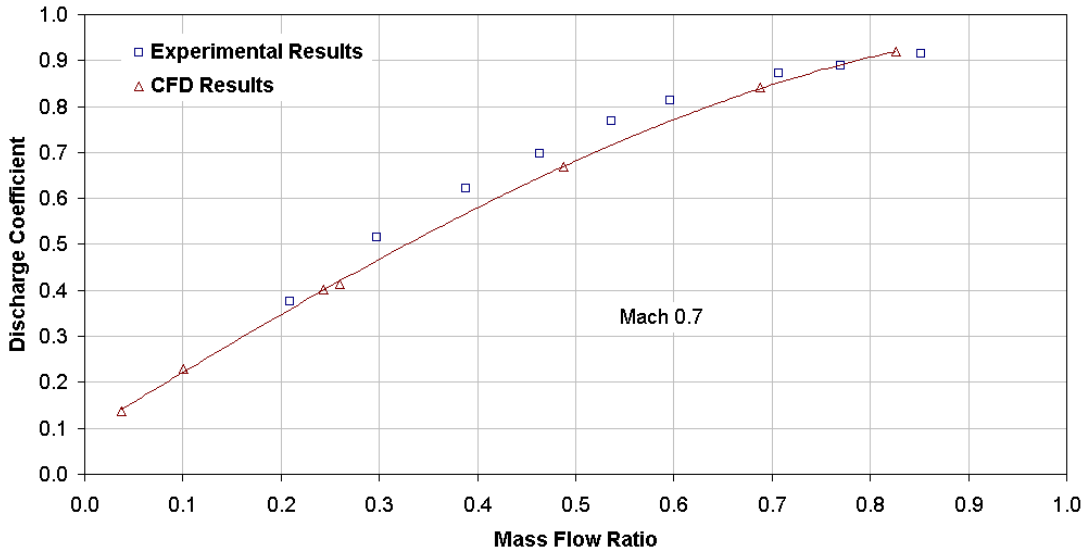

Figure 04. Discharge coefficient for an outlet without grills. Numerical and Experimental results from Dewey and Vick (1955).

The effect of varying the external flow Mach number is investigated in Fig. 05, which compares the discharge coefficients obtained from CFD analysis for Mach 0.7 and Mach 0.3.

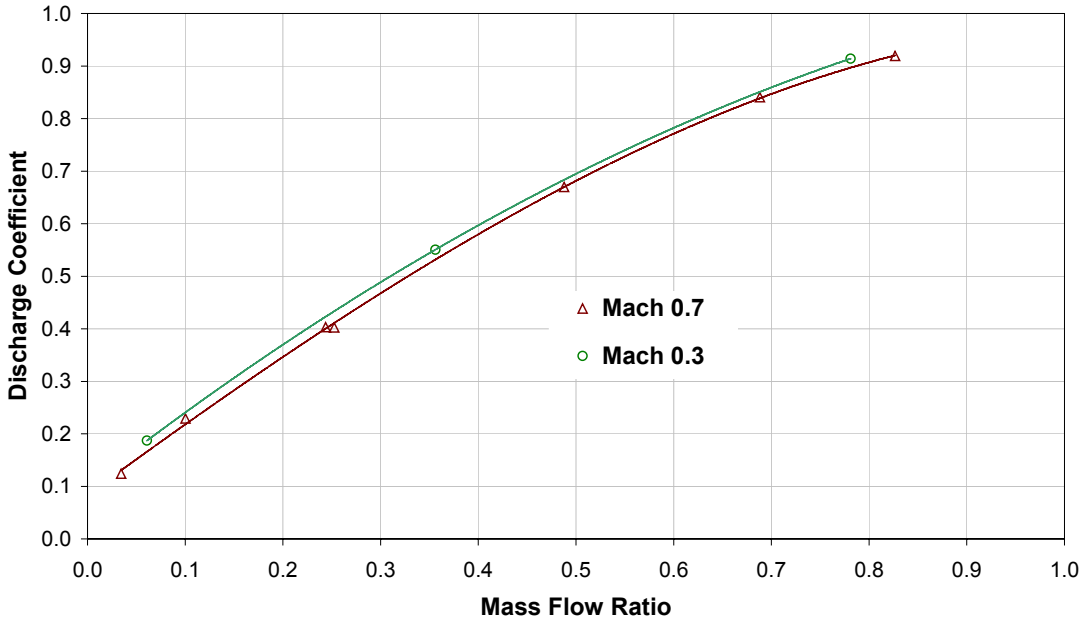

Figure 05. Discharge Coefficient for different External Flow Mach numbers – CFD Results.

It is observed that the curves of discharge coefficient as a function of the mass flow ratio are very similar for both values of Mach number. The same conclusion was found in the experimental results of Dewey and Vick (1955), but for a different Mach number range. However, it is observed that for the same total pressure at the duct inlet, a larger mass flow ratio, along with a larger discharge coefficient, is obtained in the lower Mach number case. This effect can be observed in Fig. 06 and Fig. 07, which bring contour plots of Mach number in the symmetry plane of the computational domain for the case of inlet total pressure equal to 104000Pa with Mach 0.7 (Case 01 in Tab. 01) and Mach 0.3 (Case 09 in Tab. 01).

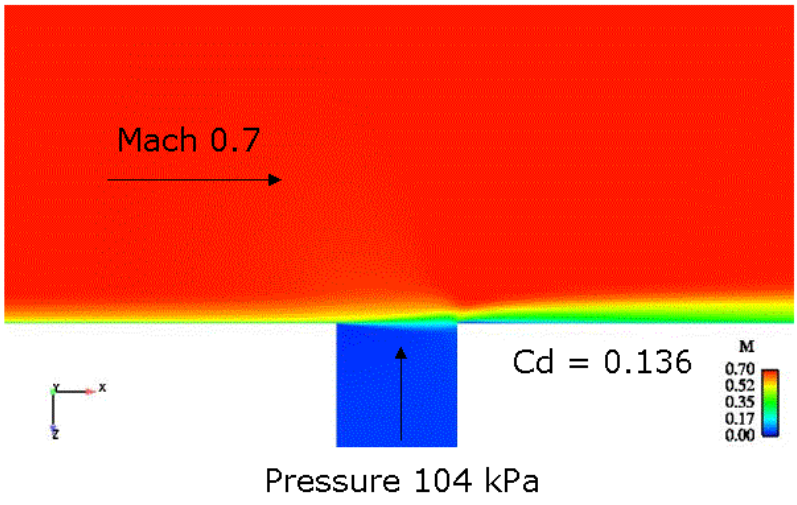

Figure 06. Mach number contours at the Symmetry Plane for Case 01.

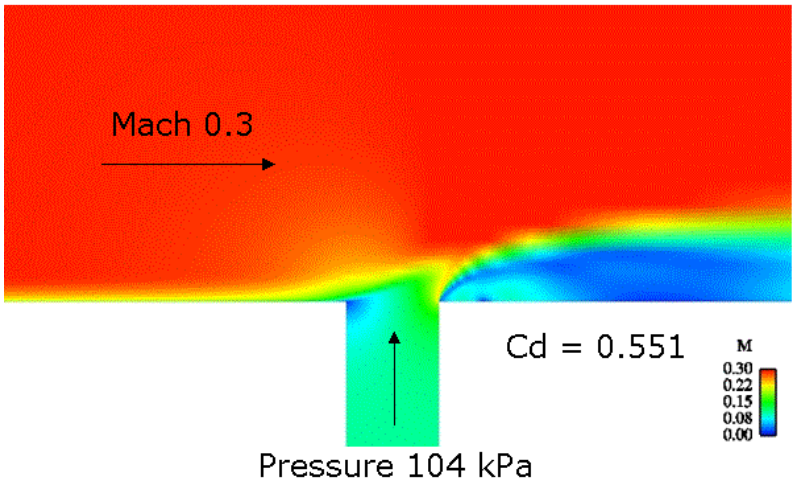

Figure 07. Mach number contours at the Symmetry Plane for Case 09.

Figures 06 and 07 clearly show that in the Mach 0.3 case the duct flow has a deeper penetration in the external freestream, which larger velocities and mass flow rate, when comparing to the Mach 0.7 condition. In addition, in the Mach 0.3 case it is observed a recirculation region behind the air outlet.

The next step of the analysis consisted in evaluating the effect of installing in the air outlets grills with turning vanes. The use of internal vanes is an attempt of increasing the discharge coefficient by means of orienting the duct flow more towards the same direction of the external flow. Cases 1, 4, 6 and 7 were run to obtain a discharge coefficient curve, which is displayed in Fig. 08 together with the previous curve of the case without a grill.

From Fig. 08, it can be observed that the results of installing a grill with internal vanes are very similar to the case without grills until a limiting value of the mass-flow ratio, where the losses caused by the vanes predominate and the discharge coefficient values are reduced when compared to the case without a grill.

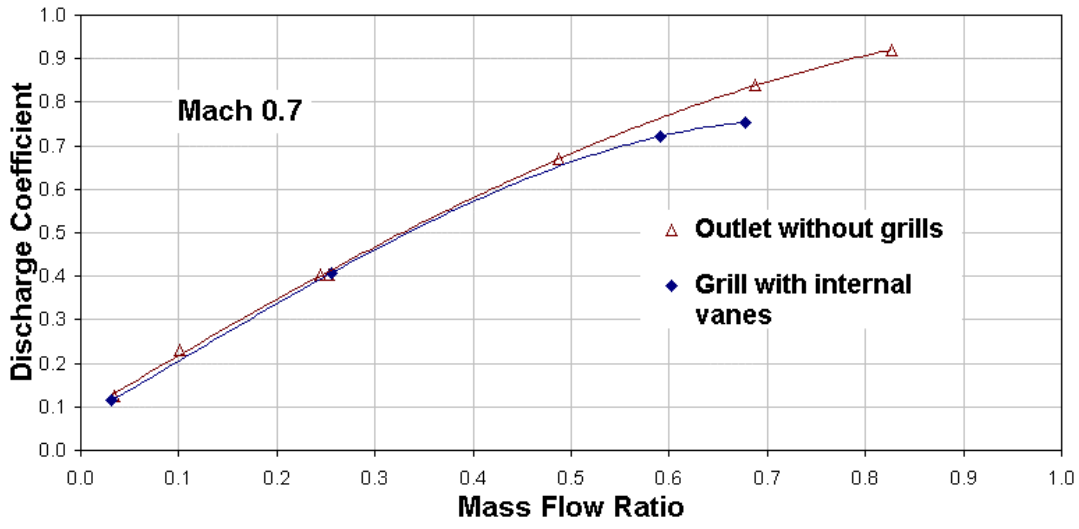

Figure 08. Discharge Coefficient for configurations without a grill and grill with internal vanes – Mach 0.7 External Flow - CFD Results.

The configuration with an external vane was analyzed in the following step. Similarly to the case with internal vanes, cases 01, 04, 06 and 07 were run and the discharge coefficient curve is shown in Fig. 09 in comparison to the case without a grill installed.

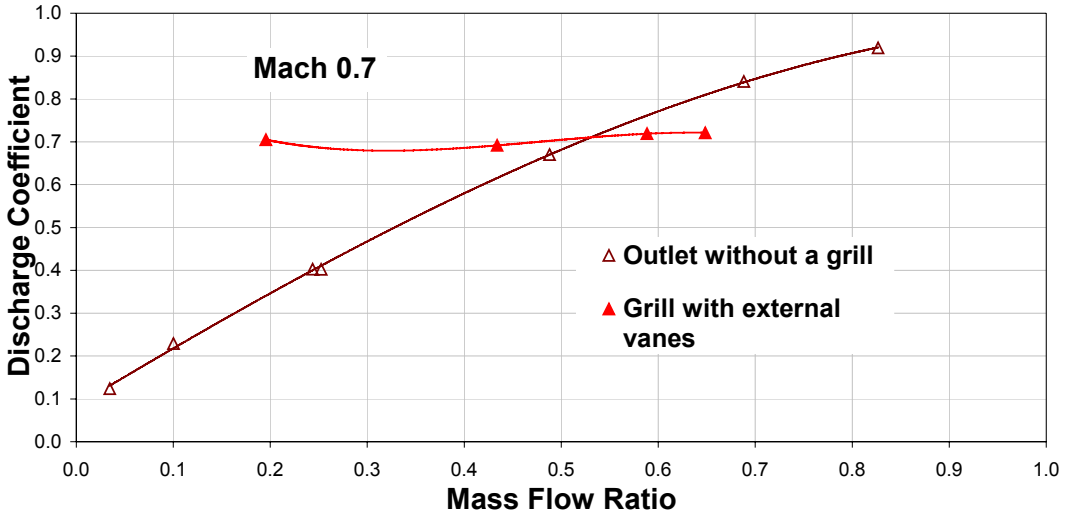

Figure 09. Discharge Coefficient for configurations without a grill and grill with external vanes – Mach 0.7 External Flow - CFD Results.

The results of Fig. 09 are quite different from what has been observed so far in the present study. It can be noticed that the suction effect created by the external vanes make the discharge coefficients curve to be nearly constant with the variation in mass flow ratio values. It is also observed that, for the grill with external vanes, the discharge coefficients are larger than those of the outlet without a grill until a limiting value of the mass flow ratio where the losses caused by the vanes are predominant and the discharge coefficient values become lower than those for the configuration without a grill. Those effects were also observed in the experimental results Dewey and Vick (1955), for a configuration of recessed outlets, which also caused suction effects.

Although the use of a grill with external vanes may be benefic for an aircraft ventilation or air-conditioning system, the benefit has to be large enough to justify the increment in aircraft drag caused by the vanes.

Figure 10 shows a comparison between this work CFD results and the experimental values of Dewey and Vick (1955) in terms of pressure coefficient at the outlet region. The pressure coefficient was measured along the main flow (M=0.7) for both the upstream and downstream regions with respect to the outlet. The longitudinal position x has been made dimensionless using the outlet-throat width t, the origin was position at the outlet center and made positive along the free stream direction. The mass flow ratio for the CFD cases investigated were chosen to match the experimental data as close as possible. The experimental mass flow ratio values are zero, 0.3, 0.6 and 0.9 while CFD results are for MFR values of 0.25, 0.49 and 0.83.

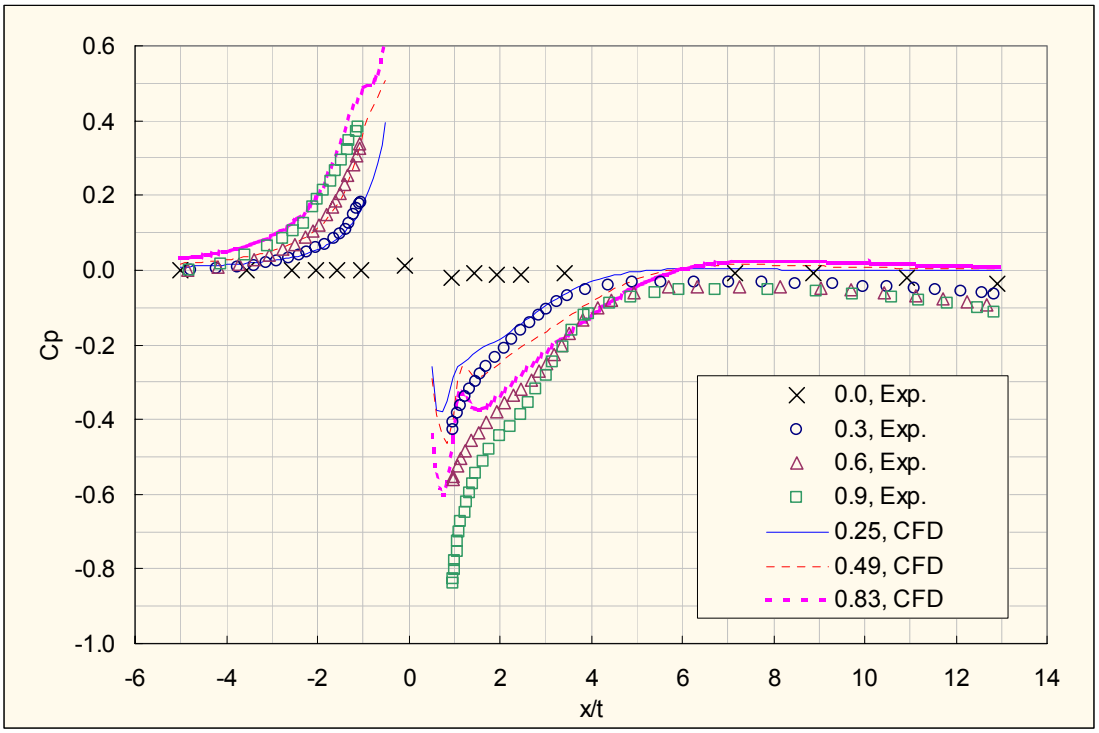

Figure 10. Comparison between this work CFD results and the experimental values of Dewey and Vick (1955). Pressure coefficients along the free stream at Mach 0.7, origin at the center of the outlet without a grill. Outlet MFR values of 0.25, 0.49 and 0.83 (CFD) and zero, 0.3, 0.6 and 0.9 (experimental).

The numerical simulation is in good agreement with the experimental values, particularly in the region upstream from the outlet ($x/t < 0$). The differences found in the downstream region ($x/t>0$) can be explained by the very complex flow pattern observed in that region, as described in Fric and Roshko (1994) and Kelso et al., (1996), that requires a more sophisticate numerical method to capture accurately that local phenomena.

4. Conclusions

In this paper it was evaluated the discharge coefficient of air outlets in the presence of an external flow by means of CFD analysis. The CFD model consisted of a rectangular duct discharging normally to a flat plate and air flowing on the plate surface. Three configurations of the duct outlet were considered: without any grill, using a grill with internal vanes and using a grill with external vanes. It was also considered two conditions of the external flow: low-speed (Mach 0.3) and high-speed (Mach 0.7).

At first, the CFD analysis was validated by comparing the discharge coefficient values obtained numerically with experimental data available in the literature for the air outlet configuration without any grill and external Mach number 0.7. A good agreement was observed in the comparative analysis. After that it was varied the external flow velocity for a Mach number 0.3. It was observed that the discharge coefficient versus mass-flow ratio curve were practically insensitive to the Mach number variation.

In a second step, it was evaluated the effect of installing a grill with either internal or external 60^o vanes in the air outlet. For the internal vanes, it was not observed any increment in the discharge coefficient values. The results were very similar to those of the case without a grill until a limiting value of the mass flow ratio where the losses caused by the vanes seem to become predominant and the discharge coefficient values became smaller than in the configuration without a grill.

In the case with external vanes it was observed that a nearly flat discharge coefficient curve was obtained. The values were substantially higher than those of the configuration without a grill, but again until a value of the mass-flow ratio where the losses caused in the duct flow by the vanes seem to become predominant.

At last, it was performed a comparison between numerical and experimental values of the pressure coefficient on the flat plate, in the regions before and after the air outlet. It was observed a good agreement in the before outlet region but a poor concordance in the aft-outlet region, indicating the need of more sophisticate CFD models to capture the complex flow pattern of that region.

The present study clearly indicate that CFD is a valuable tool for the determination of discharge coefficients of air outlets in the presence of an external flow. The results obtained can be used in the design of air outlets of aircraft air-conditioning/ventilation systems, which commonly operate at low mass-flow ratio conditions what may correspond to low discharge coefficients, depending on the outlet configuration.

Suggestions for future works include the evaluation of Reynolds number effects, as in this paper it was evaluated only the Mach number variation, the analysis of other outlet configurations and a parametric study regarding grid refinement, turbulence models and other numerical parameters.

6. References

Dewey, P. E., 1955, "A Preliminary Investigation on Aerodynamic Characteristics of Small Inclined Air Outlets at Transonic Mach Numbers", NACA Technical Note 3442, Washington, USA.

Dewey, P. E. and Vick, A. R., 1955, "An Investigation of the Discharge and Drag Characteristics of Auxiliary-Air Discharging into a Transonic Stream", NACA Technical Note 3466, Washington, USA.

Fric, T. F.and Roshko, A., 1994, "Vortical structure in the wake of a transverse jet," Journal of Fluid Mechanics, 279, pp. 1 –47.

Jesus, A.B., Damian, R. B., Oliveira, G.L., 2002, "Estudo Comparativo de Códigos Comerciais de CFD na Solução de Problemas Simples de Escoamentos Compressíveis e Incompressíveis", Proceedings of the 09th Brazilian Congress of Thermal Engineering ans Sciences, Caxambu-MG, Brazil.

Kelso, R. M. ,Lim, T. T. and Perry, A.E. , 1996, "An experimental study of round jets in cross-flow," Journal of Fluid Mechanics, 306, pp. 111 –144.

SAE, 1990, SAE Aerospace Applied Thermodynamics Manual, Aerospace Information Report AIR1 168/1.

S. Chakravarthy, T. Bose, P. Batten, S. Palaniswamy, U. Goldberg and O. Peroomian, 2000, "Convective Heat Transfer Inside Rotating Tubes," AIAA Paper No. 00-3356, 36th AIAA/ASME/SAE/ASEE Joint Propulsion Conference and Exhibit, Huntsville, Alabama, USA.